THERMAL CONDITIONS FOR STOPPING PYROLYSIS OF FOREST COMBUSTIBLE MATERIAL AND APPLICATIONS TO FIREFIGHTING

***Alena O. ZHDANOVA*[a, *], *Geniy V. KUZNETSOV*[a], *Jean Claude LEGROS*[a, b], *Pavel A. STRIZHAK*[a]**

[a] National Research Tomsk Polytechnic University, Tomsk, Russia

[b] Université libre de Bruxelles, CP 165/62, Brussels, Belgium

E-mail: zhdanovaao@tpu.ru

Five models describing heat transfer during evaporation of the water sprayed over the forest to stop fires and to cool down the pyrolysis of the bio- top layer are established and investigated by a parametric approach. It aims to improve the understanding of the behavior and the properties of the forest combustible material (FCM). A mathematical description of FCM surfaces (needles of pine and fir-tree, leaves of birch) is established. The characteristic time t_d to cool down the FCM layer below the temperature of the onset of the pyrolysis is the important parameter investigated in the present work. The effective conditions were determined allowing to reach the shortest t_d time and the lowest consumption of e.g. water to be dropped.

Keywords: *forest material, pyrolysis, stopping, thermal conditions.*

1. Introduction

In the recent years, world-wide efforts are aiming to improve equipment efficiency and develop technology used in the field of firefighting [1–7]. The goal is the understanding of the heat and mass exchange in the fire zone aiming to protect the firefighting agents and the equipment, avoiding absolutely their engulfment in flames. The efforts are aimed at the efficient use of firefighting agents and, of course, to reduce the ignition sources and to stop as fast as possible the extension of the fire zone; this extinguishing time is a very important parameter (let us note as t_d). The fast development of aerosolized technologies [3–7] with specific names – “water fog”, “water mist”, “steam curtain” and others can be explained by the wish to reduce the extinguishing time t_d. Different inclusions [6, 7] are often added into firefighting liquids for their intense evaporation in the fire zone. Also the pulsing aerosols inlet into flames (for generation of vapors during specified time) is used.

The most dangerous and large-scale fires are the forest ones [8, 9]. The local release of large water volumes or of their mixtures with different additives and inclusions are quite often used for their extinguishment. The transport of water has to be done as fast as possible and the sprayed quantities has to be accurately evaluated. Mainly this is done by helicopters and specially designed aircrafts (e.g. Canadair used daily around the Mediterranean Sea). Indeed the fires are very often developing in regions with difficult access.

Experts explain that the efficiency of this approach is reduced by the fact that aerosols are flying away by wind and turbulences induced by the aircraft. As the total embarked amount of water does not reach the intended areas oversized water volumes are dropped to meet the estimated needs. An important point which is not yet fully solved in this problem of the extinguishment of forest fire is the determination of the minimum volume of water sufficient to stop the FCM thermal decomposition reaction. There is no study of the influence of the amount of water (vapor and thin water films) on the FCM subsurface layer heated up to high temperatures. The solution of the problem of forest fire

extinguishing reduces to determining the volume of water sufficient to terminate the FCM thermal decomposition reaction. However, to date this problem has not been solved fully. There have not yet been studied the laws of the influence of water (especially vapor and thin water films) on the FCM subsurface layer heated up to high temperatures.

The purpose of the present study is to compare the conditions of heat exchange at FCM surface in order to cool down the fuel material layer below the pyrolysis temperature with amount of water accurately determined and with t_d as short as possible.

2. Definition of the problem

Different contributions to heat transfer are investigated in configuration composed initially by two layers. The bottom one contains the FCM materials which can be thermally decomposed when its temperature is higher than 500 K. Analysis of modern ideas about the pyrolysis of forest combustible materials (for example, [10–12]) revealed that typical temperatures of the start of FCM thermal decomposition lie within the range of 350–500 K. For simulation, we took the maximum temperature from this range (500 K). This approach allowed us to obtain estimates of the maximum values of t_d. The condition of FCM temperature reduction below this value was considered as decomposition termination. Initially this layer is at homogeneous temperature of 300 K. The initial temperature and fraction of material which could be thermally decomposed are calculated. The results will be used as initial conditions when solving the time dependent partial derivative equations of the model.

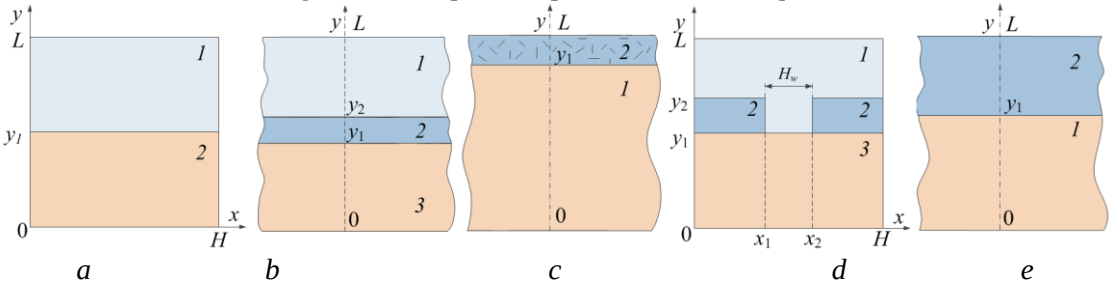

Figure 1. Heat transfer models ($0<t<t_d$): (*a*) for gas-vapor mixture above FCM: *1* – mixture of combustion products and water vapor, *2* – layer of FCM; (*b*) for homogeneous water film evaporation on FCM surface: *1* – gas-vapor mixture, *2* – water, *3* – FCM; at evaporation of water film; (*c*) for evaporation of water film: *1* – FCM, *2* – water with solid inclusions; (*d*) for two droplets on FCM surface : *1* – gas-vapor mixture, *2* – water droplets, *3* – FCM; (*e*) for water into pores of FCM: *1* – FCM layer with $T>T_d$, *2* – FCM layer with pores filled with water

We consider a few time-dependent models. The first one describes heat and mass transfer between two "layers" as sketched in Figure 1, *a*: a gas phase composed by combustion products and water vapour and the layer of FCM. An external cloud of water droplets (which is not considered in this model) is totally vaporized during its motion through the flames. It was measured [13] that the gas mixture consists of 90% water vapour and 10% combustion products. The gas phase is initially at temperature T_m and its air concentration is close to zero due to the huge injection of water vapour. The main contribution to the heat flux is produced by the endothermic vaporization of the water drops in the flame and the production of vapour and combustion products at the FCM surface. This allows to neglect the combustion of the pyrolysis products when calculating the heat transfer in the gas phase.

In the second model shown in Figure 1, *b*, a big amount of water falls through the flame and spreads over the FCM surface. The layer of liquid has a thickness L_w and is heated at its contact with the hot FCM. Vaporization takes place at this limit between the water layer and the hot FCM whose

temperature is decreased by the heat of vaporization of water. The thickness of the liquid layer is decreasing by the intense vaporization.

In the third model presented in Figure 1, *c* leaves, needles, tree branches, tree barks are lying on the FCM surface, mixed with water and forming a heterogeneous layer of water with solid inclusions, its high temperature $T>>T_d$ (T_d is the temperature of the onset of the pyrolysis reaction) produces a large water vapor cloud.

In the fourth model shown in Figure 1, *d* we took into account the interaction of separate drops with the intensively pyrolyzing FCM. Indeed water is not anymore a continuous layer; instead we consider two separated drops lying on the surface of the intensively decomposing FCM. The heat transfer occurs between separated drops which reach the FCM surface. The distance between droplets ($H_w = x_2 - x_1$) on the FCM surface is the variable parameter of the problem. The vaporization rate of all water droplets is evaluated with the appropriate thermal conditions.

In the fifth model two possible mechanisms of heat transfer in the vicinity of the FCM/water boundary were analyzed considering FCM as a porous layer (see: Fig. 1 e). At the first step the heat transfer and the phase change were investigated during motion of water into the pores of the FCM. The temperature of the layer was increased up to $T>T_d$. It was assumed that the gas-vapor mixture is formed above the FCM surface at a temperature corresponding to value measured [14, 15] inside large water clouds (300 K<T<350 K). In a second step the simulation was conducted for system in which the water filled all the pores of FCM layer and a water film is formed above this layer. It was assumed that vaporization takes place at $y=y_1$ reducing the temperature of the FCM.

An important parameter in our study is t_d the time necessary to cool down the FCM layer at temperature lower than T_d and to stop pyrolysis and its production of flammable gases. This parameter t_d was investigated with the model represented by Figure 1, *c* (water + solid inclusions). The thickness of the FCM layer with filled pores influences t_d and the exchange with the water vapour cloud above the FCM (fig. 1, *e*). The different contributions to the total heat transfer are studied with the simplification assumption that all physical properties are not depending on temperature. This is justified as the heat conductivity (λ), heat capacity (C), and density (ρ) vary by only 10-15 % [16–19] for our different components between the temperature limits.

3. The mathematical model

3.1. System of equations

Energy balance equation for FCM ($0<x<H$, $0<y<y_1$)

$$\rho_3 C_3 \frac{\partial T_3}{\partial t} = \lambda_3 \left(\frac{\partial^2 T_3}{\partial x^2} + \frac{\partial^2 T_3}{\partial y^2}\right) + Q_3 W_3 ; \quad (1)$$

Arrhenius equation for pyrolysis reaction in FCM (one component is produced) ($0<x<H$, $0<y<y_1$)

$$\frac{d\varphi_3}{dt} = (1-\varphi_3) k_3^0 \exp\left(-\frac{E_3}{RT_3}\right) ; \quad (2)$$

Thermal balance equation for water droplets ($0<x<x_1$, $x_2<x<H$, $y_1<y<y_2$)

$$\rho_2 C_2 \frac{\partial T_2}{\partial t} = \lambda_2 \left(\frac{\partial^2 T_2}{\partial x^2} + \frac{\partial^2 T_2}{\partial y^2}\right) ; \quad (3)$$

Energy balance equation for gas-vapor mixture ($x_1<x<x_2$, $y_1<y<y_2$, $0<x<H$, $y_2<y<L$)

$$\rho_1 C_1 \frac{\partial T_1}{\partial t} = \lambda_1 \left(\frac{\partial^2 T_1}{\partial x^2} + \frac{\partial^2 T_1}{\partial y^2}\right) ; \quad (4)$$

Diffusion equation for pyrolysis products of FCM ($x_1<x<x_2$, $y_1<y<y_2$, $0<x<H$, $y_2<y<L$)

$$\frac{\partial C_\mathrm{f}}{\partial t} = D_{11}\left(\frac{\partial^2 C_\mathrm{f}}{\partial x^2} + \frac{\partial^2 C_\mathrm{f}}{\partial y^2}\right); \tag{5}$$

Diffusion equation of water vapor in combustion product ($x_1<x<x_2$, $y_1<y<y_2$, $0<x<H$, $y_2<y<L$)

$$\frac{\partial C_\mathrm{v}}{\partial t} = D_{12}\left(\frac{\partial^2 C_\mathrm{v}}{\partial x^2} + \frac{\partial^2 C_\mathrm{v}}{\partial y^2}\right). \tag{6}$$

3.2. Boundary conditions

The corresponding boundary conditions at $0<t<t_\mathrm{d}$ (Fig. 1,*d*) are:

$x=0$, $x=H$, $0<y<y_1$ $\qquad \frac{\partial T_3}{\partial x} = 0$; (7)

$x=0$, $x=H$, $y_1<y<y_2$ $\qquad \frac{\partial T_2}{\partial x} = 0$; (8)

$x=0$, $x=H$, $y_2<y<L$ $\qquad \frac{\partial T_1}{\partial x} = 0$, $\frac{\partial C_\mathrm{v}}{\partial x} = 0$, $\frac{\partial C_\mathrm{f}}{\partial x} = 0$; (9)

$y=0$, $0<x<H$ $\qquad \frac{\partial T_3}{\partial y} = 0$; (10)

$y=y_1$, $0<x<x_1$, $x_2<x<H$ $\qquad -\lambda_3\frac{\partial T_3}{\partial y} - Q_3 W_3^{\Sigma} - Q_2 W_2 = -\lambda_2\frac{\partial T_2}{\partial y}$; (11)

$y=y_1$, $x_1<x<x_2$ $\qquad -\lambda_3\frac{\partial T_3}{\partial y} - Q_3 W_3^{\Sigma} = -\lambda_1\frac{\partial T_1}{\partial y}$, $\frac{\partial C_\mathrm{f}}{\partial y} = \frac{W_3^{\Sigma}}{\rho_{11} D_{11}}$, $\frac{\partial C_\mathrm{v}}{\partial y} = 0$; (12)

$x=x_1$, $x=x_2$, $y_1<y<y_2$ $\qquad -\lambda_2\frac{\partial T_2}{\partial x} - Q_2 W_2 = -\lambda_1\frac{\partial T_1}{\partial x}$, $\frac{\partial C_\mathrm{v}}{\partial x} = \frac{W_2}{\rho_{12} D_{12}}$, $\frac{\partial C_\mathrm{f}}{\partial x} = 0$; (13)

$y=y_2$, $0<x<x_1$, $x_2<x<H$ $\qquad -\lambda_2\frac{\partial T_2}{\partial y} - Q_2 W_2 = -\lambda_1\frac{\partial T_1}{\partial y}$, $\frac{\partial C_\mathrm{v}}{\partial y} = \frac{W_2}{\rho_{12} D_{12}}$, $\frac{\partial C_\mathrm{f}}{\partial y} = 0$; (14)

$y=L$, $0<x<H$ $\qquad \frac{\partial^2 T_2}{\partial y^2} = 0$, $\frac{\partial^2 C_\mathrm{v}}{\partial y^2} = 0$, $\frac{\partial^2 C_\mathrm{f}}{\partial y^2} = 0$. (15)

The evaporation rate was calculated according to formula reported in [20]:

$$W_2 = \frac{\beta}{1 - k_\beta \beta}\frac{(P^\mathrm{n} - P)}{\sqrt{2\pi R T_{2s} / M}}. \tag{16}$$

Non-dimensional parameters β and k_β were taken equal to 0.1 and 0.4 [14, 15].

To calculate the FCM mass rate of pyrolysis, we used [18]:

$$W_3 = \varphi_3 \rho_3 k_3^0 \exp\left(-\frac{E_3}{R T_3}\right). \tag{17}$$

The water vapor pressure was calculated according to Clausius - Clapeyron equation [18].
The algorithms and methods are described in previous publication [21] they were used to account the injection from under the droplets of water vapors and thermal decomposition products in the system presented in Figure 1, *d*. The thermophysical characteristics of FCM were calculated taking into account their changes during pyrolysis:

$$\lambda_3 = \lambda_{31}\varphi_3 + \lambda_{32}\left(1-\varphi_3\right);\ C_3 = C_{31}\varphi_3 + C_{32}\left(1-\varphi_3\right);\ \rho_3 = \rho_{31}\varphi_3 + \rho_{32}\left(1-\varphi_3\right). \tag{18}$$

3.3. Initial conditions

Initial (t=0) conditions (fig. 1, *d*): $T=T_0(x, y)$ and $\varphi_3=\varphi_0(x, y)$ at $0<x<H$, $0<y<y_1$; $T=T_\mathrm{w}$ at $0<x<x_1$, $x_2<x<H$, $y_1<y<y_2$; $T=T_\mathrm{m}$; C_v=0; C_f=0 at $x_1<x<x_2$, $y_1<y<y_2$, $0<x<H$, $y_2<y<L$. Here $T_0(x, y)$, $\varphi_0(x,$

y) are the initial distributions of temperature and fraction of substance which can be decomposed in the FCM. The initial distribution of temperature $T_0(x, y)$ and the fraction of substance $\varphi_0(x, y)$ which can be decomposed in the FCM layer (with thickness L_f) were calculated. The condition

$$\lambda \frac{\partial T}{\partial y} = \alpha(T_g - T_0)$$

was accepted on the border "FCM – external area" (T_g=1170 K, α= 10 W/(m^2 K)). This conditions are corresponded to real fires [21, 22]. In this configuration, Figure 2 shows the initial distributions of $T_0(x, y)$ and $\varphi_0(x, y)$ in the FCM layer (leaves of birch, needles of pine and fir-tree were regarded) and will be used to solve the equation of energy in the FCM layer [21]. T_0 and $\varphi_0 \rightarrow 0$ are taken constant along the x-axis.

Under thermal decomposition conditions, the coefficients of thermal conductivity (λ), heat capacity (C), and density (ρ) vary between 10–15% for the tested FCM [10–12]. Therefore, we can estimate the main integral parameter assuming that λ = const, C = const, ρ = const. The parameter φ_3 represents the proportion of a substance capable of chemical reaction, i.e. thermal decomposition. Since the proportion of reacting FCM decreases during pyrolysis (gaseous products of pyrolysis are released and coke residue is formed during thermal decomposition), the values of FCM thermophysical characteristics are recalculated at each time step, according to the change of φ_3. In other words, the model takes into account how much gas or coke residue is in the FCM structure.

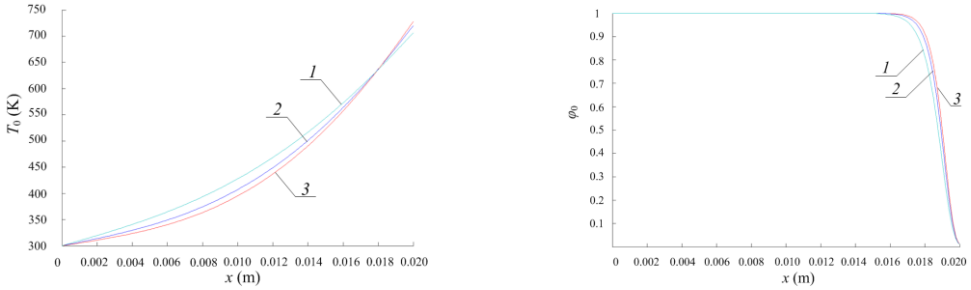

a *b*

Figure 2. Distributions of temperature (*a*) and fraction of substance which can participate into chemical reactions (*b*) in a FCM layer 2 sm thick (L_f=0.02 m). Three FCM components: *1* – leaves of birch, *2* – needles of pine, *3* – needles of fir-tree

3.4 Numerical simulation methods

The system of nonlinear time-dependent differential equations (1) – (18) was solved by finite difference method. The discretized equations were solved by locally-one-dimensional method. The sweep method using implicit four points difference scheme was applied to solve the one-dimensional difference equations. Discretized equations were solved by iteration method [23]. Different time steps (10^{-4}–10^{-2} s) and non-uniform node densities in space (10^{-8}–10^{-6} m) were used to improve the accuracy of the solutions of equations (1)–(18). The grid was refined by an algorithm similar to the method used in vicinity of phase transition boundaries [21]. The confidence estimation procedure of theoretical investigation results is based on conservative estimations of the applied difference scheme as we previously validate [21].

3.5 Results

3.5.1 The model "combustion products + water vapor/FCM layer"

Numerical investigations were conducted with values of parameters given here after [16–19]. The initial temperature of FCM boundary layer $T_0(x, y)$ and fraction of substance $\varphi_0(x, y)$ which can

participate in the chemical reaction (thermal decomposition) were calculated separately [21] and are given in Figure 2. The thermal decomposition is starting in FCM at T_d=500 K. The parameters of chemical reactions in the FCM are: k_2^0=3.63·104 [s^{-1}]; E_2=78.114 [kJ/mole]; Q_2=10^3 [J/kg]. Non-dimensional condensation (evaporation) coefficient is β=0.1. Molar mass of water is M=18 [kg/kmole]. The energy absorbed by water evaporation is Q_e=2.26 [MJ/kg] with initial temperature of water and gas-vapor temperature T_m=300 K. The thickness of the FCM boundary layer was varied in the range of L_f=0.02–0.06 m.

Thermophysical characteristics of the involved substances (temperature 300 K and pressure 101.3 kPa) were taken as in [10–12, 16–19] and presented in Table 1.

Table 1. Thermophysical characteristics of the involved substances

	Heat conduction (λ), [W/(m·K)]	Heat capacity (C), [J/(kg·K)]	Density (ρ), [kg/m^3]
Leaves of birch	λ_{31}=0.125; λ_{32}=0.029	C_{31}=1719; C_{32}=2449	ρ_{31}=614; ρ_{32}=2.7
Pine needles	λ_{31}=0.102; λ_{32}=0.027	C_{31}=1400; C_{32}=2280	ρ_{31}=500; ρ_{32}=2.5
Fir-tree needles	λ_{31}=0.091; λ_{32}=0.024	C_{31}=1246; C_{32}=2026	ρ_{31}=445; ρ_{32}=2.2
Water	λ_2=0.56	C_2=4200	ρ_2=1000
Gas-vapor mixture	λ_1=0.026	C_1=1190	ρ_1=1.161

The gas-vapor mixture temperature was varied in the range 280<T_m<340 K inside the "mixture of combustion products and water vapors/FCM boundary layer" system (see: Figure 1, *a*). The thickness of the FCM boundary layer was varied in the range 35<L_f<80 mm. Dimensions of the solution domain were changed according to L_f values in ranges 0.1<H<0.5 m, 0.1<L<0.5 m.

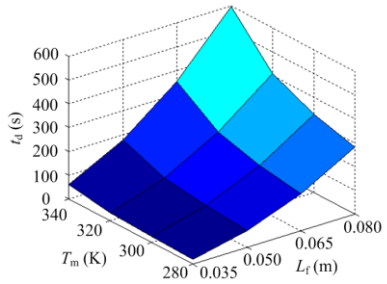

Figure 3. t_d of FCM according to its layer thickness L_f and T_m the gas-vapor mixture temperature for the model "combustion products + water vapor/FCM layer"

Parameter t_d is the time needed to cool down the FCM below the temperature T_d at which he starts to be decomposed by heat. The surface corresponding to this dependence of t_d on T_m and on thickness of the FCM boundary layer (L_f) is given in Figure 3.

This surface t_d = $f(T_m, L_f)$ obtained by our numerical investigations is an important result giving the conditions to stop the thermal decomposition in FCM. Thus, the values of T_m and L_f parameters corresponding to the time t_d located on this surface or below characterize the conditions of stopping the thermal decomposition of FCM i.e. to stop combustible source.

3.5.2 The model "water film/FCM"

The numerical investigations of the model "water film/FCM" (see: Fig. 1b) were conducted with water film of homogeneous thickness equal to L_w=0.01 m. Dimensions of the solution domain were changed in the range 0.02<L<0.2 m according to L_f values. Figure 4, *a* shows a result of our numerical investigations: the liquid layer thickness L_e (evaporated during thermal decomposition reaction weakening) as a function of the thickness L_f. of the hot FCM layer. The L_e value is the smallest water film thickness when the temperature on FCM becomes lower than T_d.

The non-linearity of L_e with respect to L_f is mainly due to the nonlinear dependence of FCM decomposition rate on temperature [10]. The initial values of $T_0(x, y)$ and $\varphi_0(x, y)$ in the FCM have strong impact on the cooling conditions of FCM. The temperature distributions in the FCM layer

during combustion may significantly change with time. Specifically, this is related to burning-out of some amount of the boundary layer and to the filling of areas with gaseous combustion products and coke (as a consequence the fraction of a substance which can be thermally decomposed is significantly changed).

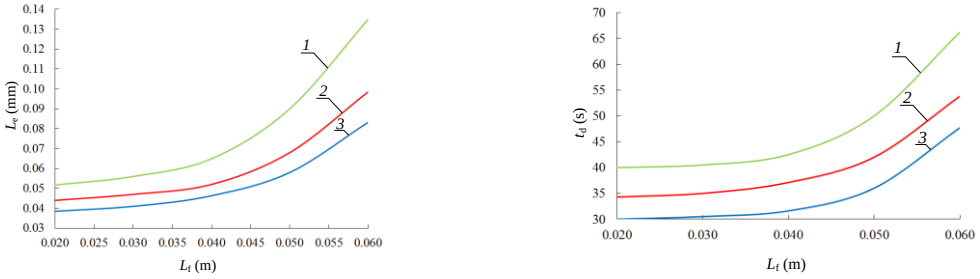

a *b*

Figure 4. (*a*) the residual thickness of liquid layer after evaporation and (*b*) the extinguishing time depending on the FCM thickness in the configuration "homogeneous water film – FCM": *1* – leaves of birch, *2* – pine needles, *3* – fir-tree needles

Profiles of $T_0(x, y)$ and $\varphi_0(x, y)$ in the Figure 2 are chosen as initial conditions for numerical simulation. Figure 2 illustrates the conditions when FCM burning-out takes place in the narrow boundary layer (before the contact with water film). In practice the thickness of the heated layer thickness may be larger than 20 mm (as in Figure 2). In this case, thickness L_e, which is required for extinguishing, will be bigger. The analysis of Figure 4 allows drawing the conclusion that liquid films with L_e not thicker than 1 mm are needed for stopping pyrolysis in FCM layers with sizes up to 0.06 m. It makes visible the oversized water supplied by the aviation approach and local dropping when liquid films thickness significantly exceeds the sufficient L_e values formed on the FCM surface.

Furthermore the extinguishing time t_d of the FCM under investigation has impacts on the water film (see: Figure 4, *b*). This is an important result obtained with our numerical simulations.

It was shown that the values of t_d do not exceed 60 s for L_f less than 0.05 m and t_d less than 90 s are needed for the complete stop of the pyrolysis with $L_f \rightarrow 0.06$ mm. The obtained results allow drawing the conclusions that water film evaporation L_e during a very small time interval is large enough for stopping the pyrolysis of FCM even with a thin liquid film L_w.

Between the values of parameters used to solve the problem the main contribution is coming from the decomposition kinetics (E_3, k_3^0, Q_3, T_d) and have significant influence on t_d and L_e values. All values of E_3, k_3^0, Q_3 and T_d are scattered in a range of 30–40 % for a wide group of typical FCM [11, 12]. The calculations presented in this work are performed with mean values for E_3, k_3^0, Q_3, T_d. The developed model of heat transfer can be used to calculate the necessary and sufficient water film thicknesses and their evaporation times for different E_3, k_3^0, Q_3 and T_d.

3.5.3. The model "water with solid inclusions/FCM"

Along with extinguishing water, bark, leaves, branches and other parts of forest can fall on the surface of FCM, which is under thermal decomposition. In this case, near the surface of FCM the heterogeneous system is formed. This system includes water, leaves, needles and bark. This system is like a "buffer layer" between the surface of thermally decomposed material and environment.

Investigations were also performed with the model "water with solid inclusions/FCM" which is described in Figure 1, *c*. The heat transfer coefficient $5<\alpha<40$ W/(m^2 K) corresponds to conditions not only of FCM surface water cooling but take also into account the air effects. The temperature

inside large water clouds was taken as T_m =350 K and the "buffer layer" thickness 0.002<$L_{w\text{-}f}$<0.01 m. The dimensions of the solution domain were changed according to values of L_f and $L_{w\text{-}f}$ in the range 0.04< L<0.12 m.

The time t_d dependence on the thickness of the FCM layer heated up to temperatures T>>T_d and with a size $L_{w\text{-}f}$=0.01 m. These functions are coming directly from our numerical investigations and are reported in Figure 5, *a*. It can be noted that t_d time is changed significantly by the variation of L_f in a typical range 0.02<L_f<0.06 m for firefighting practice. The value of t_d increases non-linearly with L_f. As an example, t_d time is increased by 10 s in the range from 0.02<L_f<0.04 m. The growth of t_d is 25 s when L_f=0.02 mm is increased up to L_f=0.06 m. This result can be explained by the different heat content of FCM layer with different L_f [21]. The dependences of t_d for different FCM as functions of "buffer layer" thickness ($L_{w\text{-}f}$) when L_f=0.04 m are reported in Figure 5, *b*.

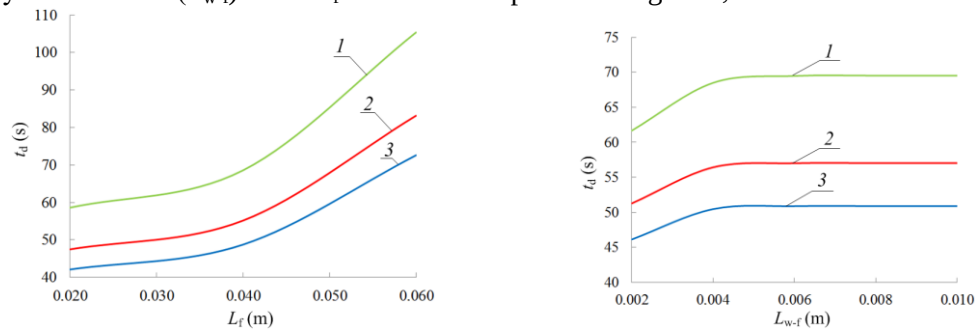

a *b*

Figure 5. Using the model "water with solid inclusions/FCM" t_d is calculated as function of thickness of the reacting FCM layer with $L_{w\text{-}f}$=0.01 m, γ=0.5, α=20 W/(m^2·K) (*a*) and t_d time depends on "buffer layer" thickness with L_f=0.04 m, γ=0.5, α=20 W/(m^2·K) (*b*) for: *1* – leaves of birch, *2* – pine needles, *3* – fir-tree needles

The t_d time increases significantly when $L_{w\text{-}f}$ increases from 0.002 m to 0.004 m. But the times t_d remain practically constant (variations are less than 1 %) when $L_{w\text{-}f}$ is increased. This result can be explained by the small mass of water evaporating during the pyrolysis slowing down. It was established that the "buffer layer" is heated-up on a depth of less than 0.005 m and the residual water layer thickness after evaporation is about 0.001 m. Therefore, an increase of $L_{w\text{-}f}$ of 0.005 m does practically not influence the conditions of FCM cooling and its t_d time. The dependence of t_d on the coefficient γ is presented in Figure 6, *a* (L_f=0.04 m, $L_{w\text{-}f}$=0.01 m and α=20 W/(m^2·K)).

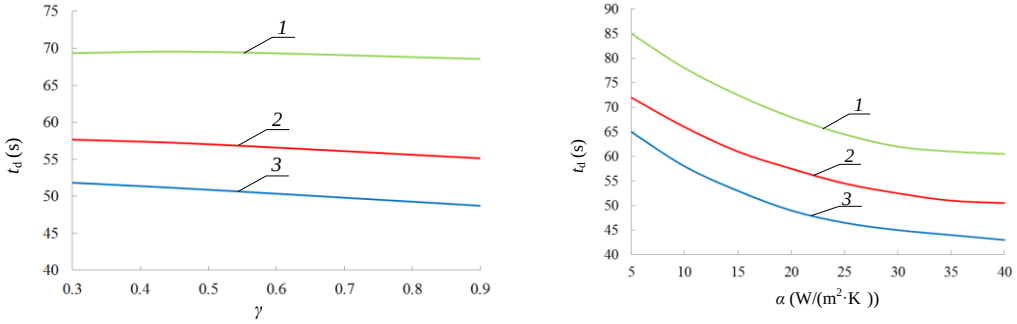

a *b*

Figure 6. Variations of t_d of configuration "water with solid inclusions – FCM" as a function of the γ coefficient when L_f=0.04 m, $L_{w\text{-}f}$=0.01 m, α=20 W/(m^2·K) (*a*) and variations of t_d time with α the heat exchange coefficient with L_f=0.04 m, $L_{w\text{-}f}$=0.01 m, γ=0.5 (*b*): *1* – leaves of birch, *2* – pine needles, *3* – fir-tree needles

It was established that the variations of parameter γ influence moderately (less than 1 %) the cooling of thermal decomposing FCM. This can be explained because water has a high vaporization enthalpy ($2 \cdot 10^6$ J/kg) and thus only a small water fraction is evaporated (e.g. the thickness of the evaporated water layer is less than 0.001 m at γ=0.5).

Figure 6, *b* shows the t_d time as a function of the heat exchange coefficient α. Mainly this coefficient depends on flow velocity v (m/s) in large water clouds. The heat exchange coefficient α is not larger than 8 W/(m^2·K) when velocities are v<1 m/s (corresponding to natural convection conditions). The heat exchange coefficient α can increase up to 40 W/(m^2·K) for higher velocities v in forced convection conditions. The increase of heat exchange at the "large water cloud/water with solid inclusions" boundary (characterized by the growth of α) leads to some decrease of t_d time. However, under α=30–40 W/(m^2·K), the change of t_d is sufficiently small (10 %). To conclude that the influence of α on the t_d decreases. The intensification of convection in the external gas-vapor mixture (for example, due to wind intensification) does not significantly influence the suppression conditions of the FCM thermal decomposition. The "buffer layer" plays the main role.

3.5.4 The model "group of water droplets FCM"

Investigations were performed with gas-vapor mixture at temperatures 300<T_m<800 K using the model "group of water droplets/FCM" (see: Figure 1, *d*). Figure 7 shows t_d time as a function of T_m in large water cloud when L_f=0.04 m and H_w=0.015 m. The non-linear dependence is due not only because the chemical reaction takes place in the hot FCM layer, but also is due to the intensive evaporation in the vicinity of the FCM surface.

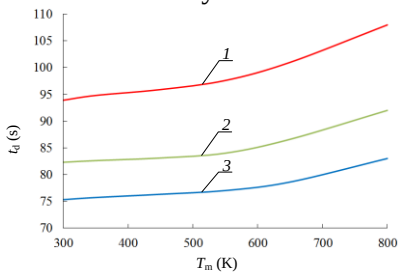

Figure 7. The t_d time for the model "group of water droplets/FCM" as function of T_m when L_f=0.04 m, H_w=0.015 m for: *1* – leaves of birch, *2* – pine needles, *3* – fir-tree needles

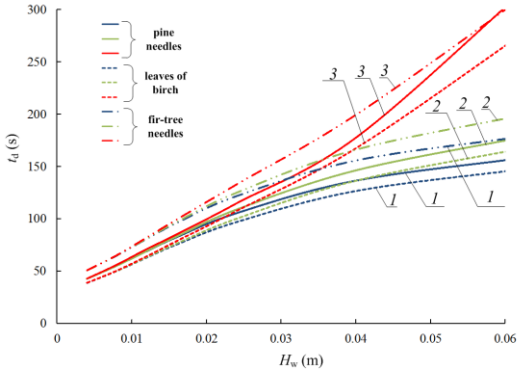

Figure 8. The t_d as function of H_w at different temperatures T_m and L_f=0.04 m for the model "group of water droplets/FCM" with *1* – T_m=300 K, *2* – T_m=450 K, *3* – T_m=800 K

Figure 8 shows t_d for FCM depending on the distance between two liquid droplets (H_w) at different temperatures in large water cloud. It can be noted that t_d time is nonlinearly reduced as H_w decreases. Also, it is worth to note the decrease of t_d with the gas-vapor mixture temperature T_m. Thus, t_d=f(H_w) are similar (curves 1, 2 are practically superposed) when T_m corresponds to the temperature of the typical large water cloud (300–450 K). However the curves 3 are significantly separated (t_d times vary by more than by 30–40 %) at T_m>450 K and H_w distance increase up to 0.06 m.

It was established that thermal decomposition reaction is not suppressed at T_m>800 K and H_w>0.06 m ($t_d \to \infty$). Therefore, values of T_m=800 K and H_w=0.06 m can be considered as the highest limit for the investigated model (see: Figure 1, *d*).

In Figure 8 the curves 1–3 are superposed when H_w<0.02 m. This result shows that conditions to slow down the pyrolysis are met even with rather high temperatures in the external gas-vapor environment. The heat of vaporization of two adjoining water droplets when the evaporation is large enough to absorb energy accumulated in hot layer of FCM and to stop pyrolyzing in the whole range of the possible variation of T_m during the same t_d time for H_w=0.02 m.

3.5.5. The model "water in pores of FCM/FCM"

The investigations with the model "water in pores of FCM layer/FCM" (see: Figure 1, *e*) were carried out with the heat exchange coefficient $10<\alpha<30$ W/(m^2·K). The temperature in large water cloud was $300<T_m<350$ K. Thickness of the FCM layer with water in pores was $0.001<L_{w\text{-}h}<0.003$ m. The characteristic dimensions of the solution domain were changed in the range of $0.04<L<0.12$ m according to the values of L_f and $L_{w\text{-}h}$. The FCM (leaves of birch, needles of pine and fir-tree) t_d times depending on layer thickness of FCM with water in pores ($L_{w\text{-}h}$) when L_f=0.04 m (see: Figure 9) were calculated with the model presented in Figure 1, *e*.

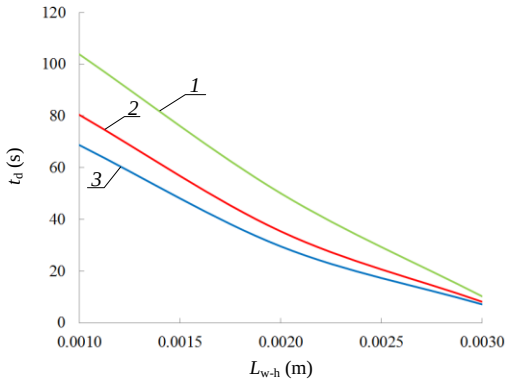

Figure 9. The t_d time for the model "water in pores of FCM layer/FCM" as a function of thickness of "FCM + water" layer with L_f=0.04 m for : *1* – leaves of birch, *2* – pine needles, *3* – fir-tree needles

It is shown that t_d time is shorter when the variations of $L_{w\text{-}h}$ are in the range $0.001\ \text{m}<L_{w\text{-}h}<0.003$ m. This effect can be explained: $L_{w\text{-}h}$ increases the volume of water filling the pores of the FCM layer where chemical reaction velocity and heat release are the largest. A maximum of the energy produced in FCM is blocked in the liquid. This leads to significant decrease of the time t_d. A large FCM reactive layer (more than 0.003 m thickness) is intensively pyrolyzed with a relatively small value of $L_{w\text{-}h}$ (less than 0.001 m). Chemical reaction velocities are initially decreased in this area as a consequence of the coupled cooling of the FCM layer (filled with water). However, this process takes significantly larger times t_d than at $L_{w\text{-}h}\rightarrow 0.003$ m.

It should be noted that we attempted to conduct relevant experiments to verify the heat and mass transfer models developed in this study. There is a satisfactory correlation of theoretical results with experiments [24], where thermal decomposition of birch leaves and fir-tree needles was suppressed by the fine drip flow. In these experiments, a thin water film (2–4 mm) was formed on the FCM surface. Time t_d deviation of simulation results and experimental data does not exceed 40–60%. Such deviation can be considered as satisfactory, since the values of t_d are mostly dependent on kinetic coefficients (k_2^0, E_2, Q_2). Unfortunately, there are very few reliable data on these coefficients, which require complex investigations. Nevertheless, one can predict times t_d for all modes of FCM pyrolysis suppression (see: Figure 1), even with existing data using the developed models.

Conclusion

Investigations were performed, allowing to study the coupled complex processes of heat transfer and chemical reaction in different models: "mixture of combustion products and water vapors/FCM boundary layer", "homogeneous water film/FCM", "water with solid inclusions/FCM", "group of water droplets/FCM" and "water in pores of FCM boundary layer". These systems show that the increase of the vaporization intensity improves the slowing down of the pyrolysis in the FCM.

Flooding the surface of FCM with large amount of water to stop the pyrolysis can be avoided. Films with thickness of some millimeters are enough for stopping completely the FCM combustion and pyrolysis. Comparison of t_d times in configuration "mixture of combustion products and water vapors" and "homogeneous water film/FCM" systems allows drawing the conclusion that series of water dropping in the properly scheduled times and space into the fire zone is the most efficient way to stop the fire extension regarding the costs in time, extinguishing agents and human resources This will

allow intensifying the heat exchange and evaporation near the FCM surface. If the duration fights are a little bit longer with respect to massive flooding, the necessary amount of water is strongly reduced with the benefit of a reduction of aircraft flight time.

Acknowledgement

The investigation was supported by Russian Science Foundation (project 14–39–00003).

Nomenclature

C – specific heat, [J/(kg·K)]
C_v – mass fraction of water vapors, [–]
C_f – mass fraction of FCM pyrolysis products, [–]
D – diffusion coefficient, [m2/s]
E – activation energy of pyrolysis reaction, [J/mole]
FCM – forest comustible material, [–]
H_w – distance between droplets, [m]
H, L – dimensions of the numerical solution domain, [m]
H_{dr}, L_{dr} – longitudinal and transverse droplet sizes, [m]
k_3^0 – pre-exponential factor of thermal decomposition reaction, [s-1]
L_e – residual thickness of liquid layer after evaporation at td time, [mm]
L_f – the thickness of the FCM boundary layer, [mm]
L_w – water film thickness, [mm]
$L_{w\text{-}f}$ – "buffer layer" thickness, [m]
$L_{w\text{-}h}$ – thickness of the FCM boundary layer with water in pores, [m]
M – molar mass, [kg/kmole]
P – water vapor pressure in the vicinity of evaporation boundary, [N/m2]
P^n – saturated water vapor pressure, [N/m2]
Q_2 –thermal effect of evaporation, [J/kg]
Q_3 – thermal effect of thermal decomposition, [J/kg]
R – gas constant, [J/(mole·K)]
t – time, [s]
T – temperature, [K]
T_{2s} – temperature at liquid evaporation boundary, [K]
t_d – time to stop pyrolysis in FCM, [s]
T_d – temperature of the onset of FCM pyrolysis, [K]
T_m – initial temperature of gas-vapor mixture, [K]
W_2 – mass evaporation rate, [kg/(m^2·s)]
W_3 – mass thermal decomposition rate, [kg/(m^3·s)]
α – heat exchange coefficient, [W/(m^2 K)]
β – nondimensional coefficients (empirical constant) of evaporation, [–]
γ – porosity coefficient of forest combustible material, [–]
λ – thermal conduction, [W/(m·K)]
v – velocity in large water clouds, [m/s]
ρ – density, [kg/m^3]
φ_3 – maximum fraction of substance which can be decomposed by pyrolysis, [–]

Subscripts

1 – gas-vapor mixture
11 – water vapor
12 – gaseous products of thermal decomposition
2 – water
3 – forest fuel material
31 – solid products of FCM pyrolysis
32 – gaseous products of FCM pyrolysis

References

[1] McAllister, S., Critical Mass Flux for Flaming Ignition of Wet Wood, *Fire Saf. J.*, 61 (2013), pp. 200-206

[2] Korobeinichev, O.P., *et al*, Fire Suppression by Low-Volatile Chemically Active Fire Suppressants Using Aerosol Technology, *Fire Saf. J.*, 51 (2012), pp. 102-109

[3] Xiao, X.K., *et al*, On the Behavior of Flame Expansion in Pool Fire Extinguishment with Steam Jet, *J Fire Sci*, 29(4) (2011), pp. 339-360

[4] Vysokomornaya, O.V., *et al*, Experimental Investigation of Atomized Water Droplet Initial

Parameters Influence on Evaporation Intensity in Flaming Combustion Zone, *Fire Saf. J.*, 70 (2014), pp. 61-70
[5] Tang, Z., *et al*, Experimental Study of the Downward Displacement of Fire-Induced Smoke by Water Sprays, *Fire Saf. J*., 55 (2013), pp. 35-49
[6] Joseph, P., *et al*, A Comparative Study of the Effects of Chemical Additives on the Suppression Efficiency of Water Mist, *Fire Saf. J*., 58 (2013), pp. 221-225
[7] Yoshida, A., *et al*, Experimental Study of Suppressing Effect of Fine Water Droplets on Propane/Air Premixed Flames Stabilized in the Stagnation Flowfield, *Fire Saf. J*., 58 (2013), pp. 84-91
[8] Qie, J., *et al*, Experimental Study of the Influences of Orientation and Altitude on Pyrolysis and Ignition of Wood, *J. Fire Sci*., 29(3) (2011), pp. 243-258
[9] Rossi, J.L., *et al*, An Analytical Model Based on Radiative Heating for the Determination of Safety Distances for Wildland Fires, *Fire Saf. J*., 46(8) (2011), pp. 520-527
[10] Grishin, A.M., *Mathematical Modeling of Forest Fire and New Methods of Fighting them*, Publishing House of Tomsk State University, Tomsk, 1997 [in Russian]
[11] Grishin, A.M., *et al*, Comparative Analysis of Thermokinetic Constant of Drying and Pyrolysis of Forest Fuels, *Combustion and Explosion Physics J.*, 27 (1991), pp. 17-24
[12] Lautenberger, C.H., Fernando-Pello, C.A., A Model for the Oxidative Pyrolysis of Wood, *Combust Flame*, 156 (2009), pp. 1503-1513
[13] Yao, B., *et al*, Experimental Study of Suppressing Poly (Methyl Metacrylate) Fires Using Water Mists, *Fire Saf. J*., 47 (2012), pp. 32-39
[14] Vysokomornaya, O.V., *et al*, Heat and Mass Transfer in the Process of Movement of Water Drops in a High-Temperature Gas Medium, *J. Eng. Phys. Thermophys*, 86(1) (2013), pp. 62-68
[15] Strizhak, P.A., Influence of Droplet Distribution in a "Water Slug" on the Temperature and Concentration of Combustion Products in its Wake, *J. Eng. Phys. Thermophys*, 86(4) (2013), pp. 895-904
[16] Vargaftik, N.B., *et al*, *Handbook of Thermal Conductivity of Liquids and Gases*, CRC Press, Boca Raton, 1994
[17] Patel (Ed.), V., *Chemical Kinetics*, Rijeka, Croatia, 2012
[18] Frank-Kamenetsky, D.A., *Diffusion and Heat Transfer in Chemical Kinetics*, Plenum, New York, 1969
[19] Baehr, H.D., Stephan, K., *Heat and Mass Transfer*, Springer Verlag, Berlin, 1998
[20] Kryukov, A.P., *et al*, About Evaporation-Condensation Coefficients on the Vapor-Liquid Interface of High Thermal Conductivity Matters, *Int. J. Heat and Mass Transfer*, 54 (2011) 13-14, pp. 3042-3048
[21] Zhdanova, A.O., *et al*, Numerical Investigation of Physicochemical Processes Occurring During Water Evaporation in the Surface Layer Pores of a Forest Combustible Material, *J. Eng. Phys. Thermophys*, 87(4) (2014), pp. 773-781
[22] McAllister, S., *et al*. Piloted Ignition of Live Forest Fuels, *Fire Saf. J*., 51 (2012), pp. 133-142
[23] Samarskii, A.A., *The Theory of Difference Schemes*, Marcel Dekker, USA, 2001
[24] Gumerov, V.M., *et al*, Determination of Characteristic Periods of Suppression of Thermal Decomposition Reaction of Forest Fuel Material by Specialized Software, *MATEC Web of Conferences*, 37(01022) (2015), pp. 1-4